Structural damage detection based on decision-level fusion with multi-vibration signals

IOP Publishing Measurement Science and Technology
Meas. Sci. Technol. **33** (2022) 105112 (15pp) https://doi.org/10.1088/1361-6501/ac7940

Structural damage detection based on decision-level fusion with multi-vibration signals

Jiqiao Zhang[1], Zihan Jin[1], Shuai Teng[1], Gongfa Chen[1,*] and David Bassir[2,3]

[1] School of Civil and Transportation Engineering, Guangdong University of Technology, Guangzhou 510006, People's Republic of China
[2] UTBM, IRAMAT UMR 7065-CNRS, Rue de Leupe, 90010 Belfort Cedex, France
[3] Centre Borelli, ENS - Université Paris-Saclay, 4 avenue des Sciences, 91190 Gif-sur-Yvette, France

E-mail: gongfa.chen@gdut.edu.cn

Received 20 January 2022, revised 6 June 2022
Accepted for publication 15 June 2022
Published 18 July 2022

Abstract

When a structure is damaged, its vibration signals change. If a single vibration signal is used for structural damage detection (SDD), it may sometimes lead to low detection accuracy. To avoid this phenomenon, this paper presents a SDD method based on decision-level fusion (DLF) with multi-vibration signals. In this study, acceleration (ACC), strain (E), displacement (DIS), and the fusion signal of all three of these signals (ACC, E and DIS), are studied. The damage information can be extracted from the vibration signal of a structure by using convolution neural networks (CNN). The above four vibration signals are used as the inputs to train four CNN models, and each model outputs a corresponding result. Finally, a DLF strategy is used to fuse the detection results of each CNN. To demonstrate the effectiveness and correctness of the proposed method, a steel frame bridge is investigated with numerical simulations and vibration experiments. The research shows that the damage detection method based on DLF with multi-vibration signals can effectively improve the accuracy of the CNN damage detection.

Keywords: structural damage detection, decision-level fusion, convolutional neural network, vibration signal

(Some figures may appear in colour only in the online journal)

1. Introduction

Structural damage detection (SDD) is an important research task in the field of structural health monitoring (SHM) [1]. SDD aims to find defects in a structure in time, so that corresponding measures can be taken to avoid major losses due to structural damage. Early SDD mainly relies on site inspections, which cost a lot of manpower and material resources, and is only effective for any surface damage of structures. When a structure is damaged, its internal physical characteristics (stiffness, mass, damping) will be changed, which will cause its modal parameters and vibration signals to change. Therefore, the vibration-based SDD methods were proposed. The SDD methods based on vibration are divided into parametric methods and nonparametric methods [2]. The parametric SDD methods are based on modal parameters and their derivatives (natural frequency [3], mode shape [4] modal strain energy [5, 6], modal flexibility [7], modal curvature [8], etc) of the structure. The nonparametric methods directly identify structural damage from the measured vibration signals (acceleration [9], strain [10], and displacement [11]) of the structure.

Although these methods have significantly improved the accuracy of SDD, they still have many shortcomings. For example, in the actual application of the parametric methods, the modal parameters are easily affected by external factors (e.g. temperature, humidity, etc). When some structures are locally damaged, only high-order modal parameters

* Author to whom any correspondence should be addressed.

are evidently affected, which is difficult measure. For non-parametric methods, a large amount of data needs to be analyzed and processed. Sometimes, the accuracy and efficiency of damage detection are questioned due to the influence of the analyst's knowledge. Therefore, it is necessary to establish a systematic, efficient, and automatic data processing tool for extracting damage information.

Machine learning (ML) methods provide a new solution to the above-mentioned problems. At present, ML algorithms are widely used in SDD. Classic algorithms include support vector machines [12] and artificial neural networks [13]. For example, Mehrjoo *et al* [14] proposed a neural network-based SDD technology for simple truss and Louisville bridge truss. In addition, ML algorithms have also been applied to some steel frames [15], bridge models [16], and actual structures [17]. A large amount of literature shows that the quality of the ML methods largely depends on the extracted features. Feature extraction techniques such as modal estimation [18], wavelet transform [19] and principal component analysis (PCA) [20], usually lead to considerable computational complexity and costs, which hinders the use of the ML methods in real-time structural health detection operations.

As one of the classic deep learning (DL) and supervised learning algorithms, the convolution neural network (CNN) provides another new approach for SDD due to its excellent feature extraction ability. The CNN can learn to associate features with the desired output, and extract features automatically. Therefore, there is no need to extract features in advance, which means CNN algorithms perform well in complex tasks by decomposing complex tasks into simpler ones. Recently, the CNN has achieved good results in many engineering applications [21, 22], which attracts many scholars to focus on the CNN. Zhong *et al* [23] proved that the CNN could extract damage information from modal shapes. Lin *et al* [24] also found that the CNN could obtain damage information from acceleration signals. Their results show that the CNN based on acceleration signals could detect 94% of the damage. Teng *et al* [25] explained the CNN feature extraction process in structural surface defect detection. The above works show that the CNN performs well in damage detection. Sometimes, using a single vibration signal or a single modal parameter as a damage indicator cannot fully reflect the true state of a structure. In order to obtain complete information about the structure, a new method of data analysis is needed.

The data-level fusion strategy provides an advanced method for SDD. By fusing multiple signals, it may comprehensively reflect the true state of a structure, avoiding the shortcomings of incomplete information carried by a single vibration signal. Chao *et al* [26] studied an adaptive decision-level fusion (DLF) strategy for the fault diagnosis of axial piston pumps using multiple channels of vibration signals. Li *et al* [27] proposed an ensemble deep CNN model with improved D–S evidence fusion for bearing fault diagnosis. In the SHM field, the time domain and frequency domain of the bridge vibration signal are fused to detect the abnormal signal of the structure in a study [28]. The accuracy of damage detection is improved by fusing the multi-mode strain energy (MSE) of the structure [29] and the MSE with dynamic response [6], and the SDD method based on vibration theory and multi-sensor signals [30] is also implemented. As the vibration signal contains the state information of the structure [31], the vibration signal can be analyzed for SDD. The fusion of multiple vibration signals is expected to improve the detection accuracy. The existing technology uses the fusion of multiple vibration signals as the input of the CNN (i.e. data-level fusion). However, the effect of each vibration signal to detect structural damage is different, and it is impossible to know in advance which vibration signal has the best effect on damage detection.

Therefore, in order to further improve the accuracy of damage detection, a SDD method based on multiple-vibration signals and DLF strategy is proposed to overcome the disadvantages discussed above. In this research, each vibration signal is used to train a CNN model, and then a DLF is performed on the detection results of the multiple CNN models, and finally the damaged state of the structure is obtained. To validate the effectiveness of the proposed method, a steel frame bridge is investigated with numerical simulations and vibration experiments, where scenarios with a single damage and double damages are set up in the numerical simulations, and multiple damage scenarios are designed in the experiments.

2. Methods and materials

A 3D steel frame bridge is taken as the research object. The vibration signals of the structure are obtained under different damage scenarios from numerical simulations and vibration experiments, namely the ACC signal, E signal and DIS signal. Then the above signals are used as the CNN input for damage detection. The specific process is shown in figure 1.

2.1. Numerical and experimental models

The numerical model (figure 2) is established by using the finite element software package ABAQUS (SIMULIA Inc., Providence, USA). The length, width, and height of the model are 2.4, 0.3 and 0.3 m, respectively. Its density, Young's modulus, Poisson's ratio, and damping ratio are 7800 kg m^{-3}, 212 GPa, 0.3 and 0.02, respectively. The bridge frame is made of 30 mm $\times$ 30 mm $\times$ 2 mm equilateral steel angles, and the web members are 20 mm $\times$ 2 mm flat steel bars. The members are numbered S1, S2, …, and S60 (figure 2). The web bars are connected with the upper and lower chords by bolts, the model is fixed at both ends, and the beam element (B31) is adopted in the numerical simulations.

The bridge model adopted in the vibration experiments is shown in figure 3. The flat steel bars are connected by bolts, and the damage to a bar is simulated by cutting off its cross section. The equipment used in the vibration experiments (figure 4) includes: acceleration sensors (YD-2150), damaged and intact bars, force hammer (JML-03), strain gauges, dynamic data acquisition instrument (JM-3841), and PC.

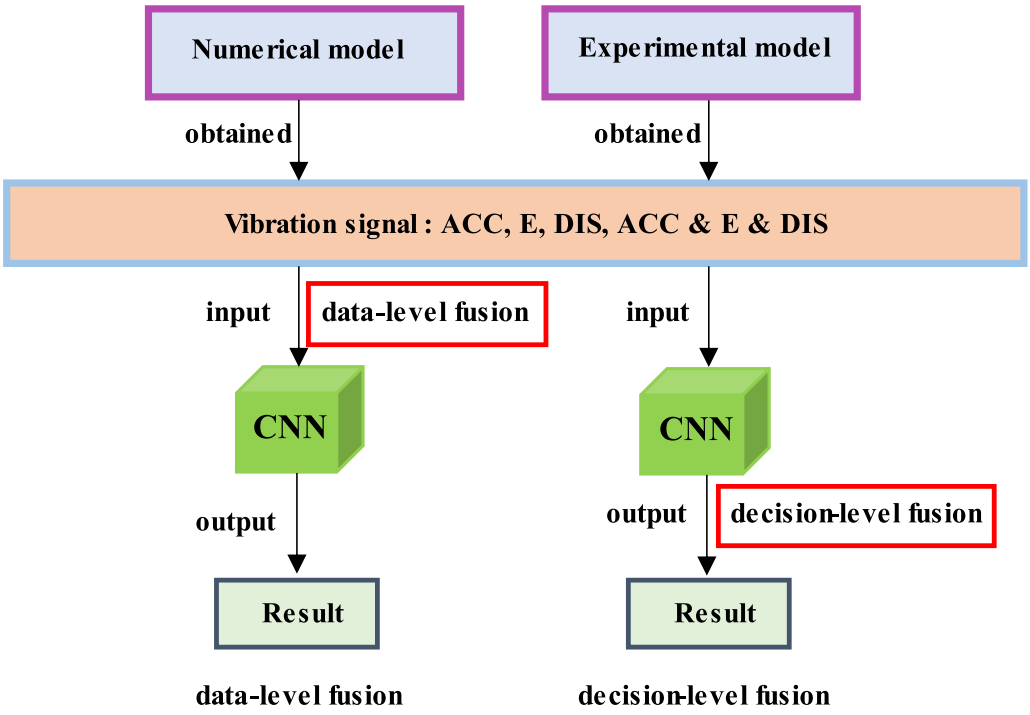

Figure 1. SSD process using CNN with data-level fusion and DLF.

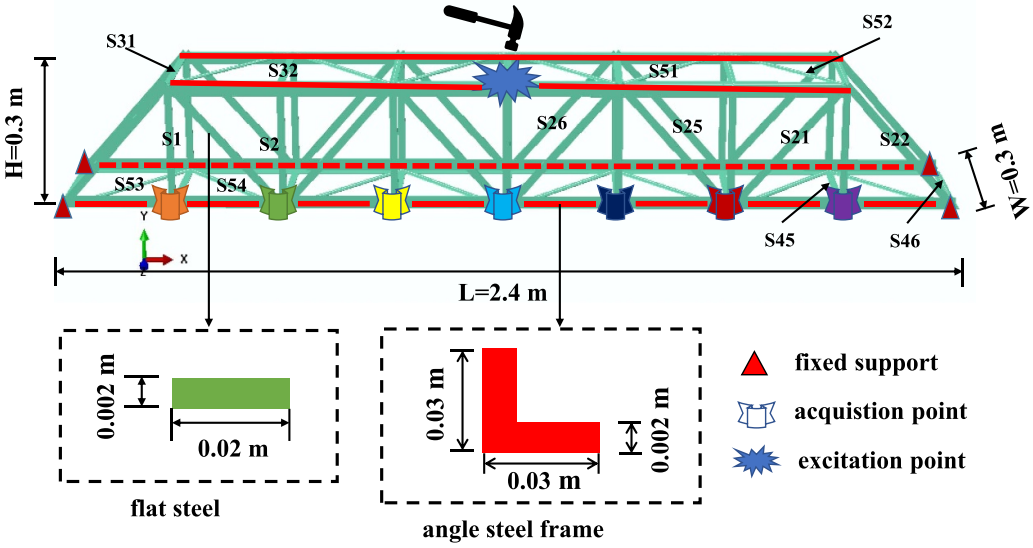

Figure 2. Numerical simulation model of the 3D steel frame bridge.

2.2. Samples obtained from numerical simulations and vibration experiments

First, impulse forces (1 kN) are applied to the structure, the excitation time is 4 s, and the sampling increment is 0.01 s. Thus, one ACC or E signal can be obtained for each excitation, which contains 400 sampling points. The vibration signals of 61 scenarios (the intact structure and 60 damaged structures) are obtained in batches through ABAQUS and Python, as shown in figure 5 (e.g. for the ACC signal). In this study, the damage is simulated as the reduction of the elastic modulus, which assumes that the reduction of the elastic modulus is proportional to the damage degree of the flat steel. For example, if the structural damage is 50%, its elastic modulus is reduced to half of its original value.

In the cases of a single damage, a total of 361 sets of data (6 damage degree $\times$ 60 bars $+$ 1 intact bar) with six damage degrees of 10%, 20%, 40%, 60%, 75%, and 90% for each bar are used as samples to train the network. A total of 61 sets of data (60 damaged structures $+$ 1 intact structure) with a damage degree of 50% are used as the testing samples to test the network.

Figure 3. Vibration experiment model of the 3D steel frame bridge.

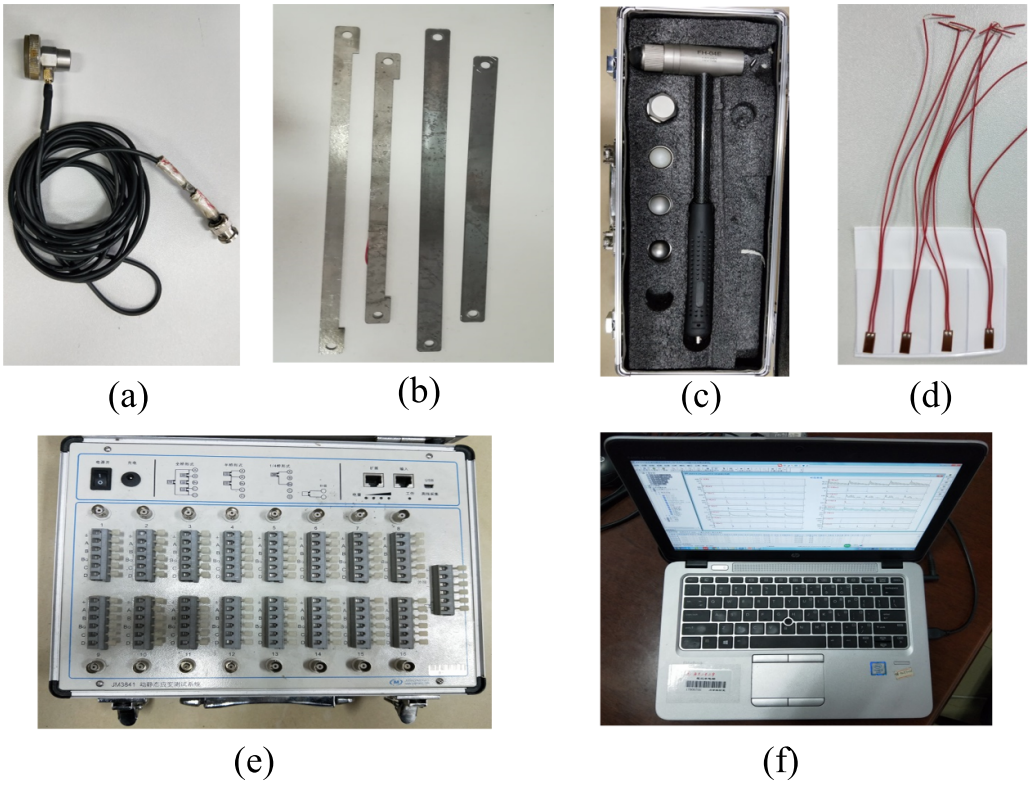

Figure 4. Experimental equipment: (a) acceleration sensor (YD-2150), (b) intact and damaged bars, (c) force hammer (JML-03), (d) strain gauge, (e) dynamic acquisition instrument (JM-3841), (f) PC.

In the case of two damages, two damaged bars are randomly selected from S3, S5, S6, S11, S18, S19, S20, S25, S34, S35, S40, S41, S42, S43, S49, S50, S51, S54 and S57 (figure 2). Each bar damage is 50%, so there are 171 (C_{19}^{2}) cases in total, 11 of which are selected as the testing sets, and the rest (160 cases) are used as the training sets. The specific testing samples are shown in table 1.

Secondly, the implementation for the vibration experiment is as follows: the ACC signals and the E signals are measured by the acceleration sensors and the strain gauges, respectively. The sampling frequency of the dynamic acquisition instrument is adjusted to 100 Hz, and the acquisition time is 60 s. The acceleration sensors are set up at seven positions at the bottom of the structure (A, B, …, G), and the strain gauges are set up on the 11 bars in the front row, as shown in figure 6. Then the

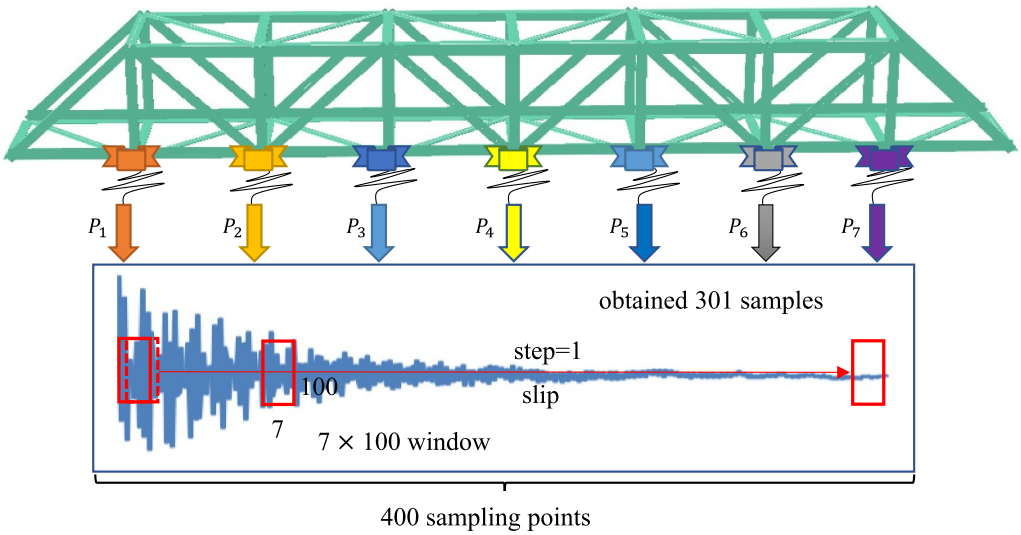

Figure 5. Acquisition of the CNN samples.

Table 1. Test samples for the scenarios with two damages.

Data number	Testing set	Data number	Testing set
E1	S3, S6	E7	S18, S19
E2	S3, S11	E8	S35, S40
E3	S3, S20	E9	S35, S42
E4	S3, S25	E10	S35, S49
E5	S3, S34	E11	S41, S43
E6	S5, S34	—	—

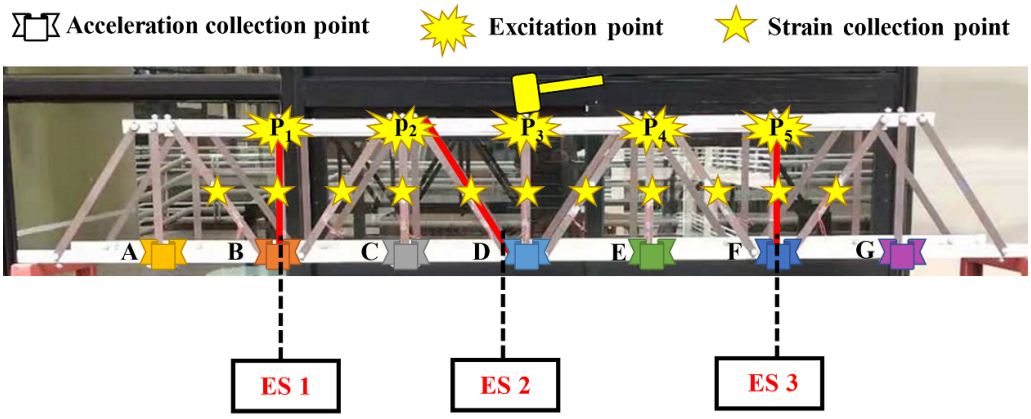

Figure 6. Placement points of the sensors and the locations of the damaged members.

model is hit six times at the excitation point with a force hammer (within 60 s). The corresponding DIS signal is obtained by integrating the original ACC signal twice.

Considering the influence of excitation points on damage detection, five excitation points were set in this study, as shown in figure 10, namely P_1, P_2, P_3, P_4 and P_5. The damage scenarios of the experiment are implemented by replacing the intact bars with damaged ones, and the specific damage scenarios are as follows (figure 8): scenario 1 (intact state), scenario 2 (ES1 damaged), scenario 3 (ES2 damaged), scenario 4 (ES3 damaged), scenario 5 (ES1 and ES2 damaged), scenario 6 (ES1, ES2 and ES3 damaged). In each scenario, the signals collected from the first four excitations are used as the training sets, and the signals collected from the last two excitations are used as the testing sets. As shown in figure 7, four CNN models (CNN1, CNN2, CNN3, and CNN4) are trained with the four vibration signals (ACC, E, DIS, and ACC & E & DIS), respectively.

Since the amount of acquired data is relatively small, the sample augment technology can be used to expand the test samples as more training samples make the CNN prediction better. One acceleration signal can be obtained for each

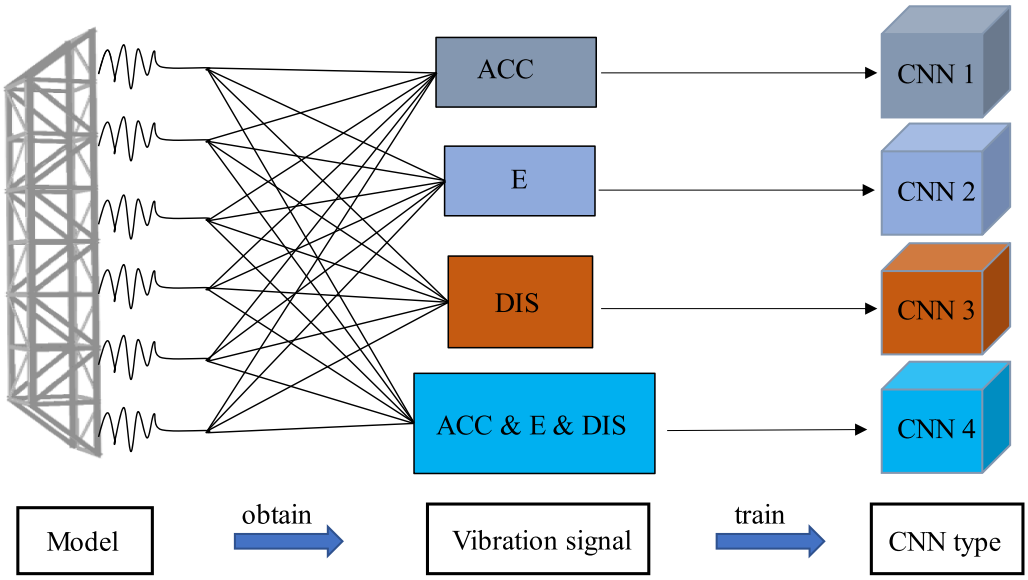

Figure 7. CNN training with vibration signals.

Table 2. CNN samples obtained from experiments.

Damage scenarios	Scenario	Number of training samples	Number of test samples
SD1	Intact	1204	602
SD2	ES1		
SD3	ES2		
SD4	ES3		
SD5	ES1, ES2		
SD6	ES1, ES2, ES3		

excitation, which contains 400 sampling points. For the six excitations, there are six such acceleration signals. The specific augment steps are as follow (figure 5): a 100 × 7 sliding window is used along the time direction, and the sliding step is one point, so that each signal can produce 301 samples, and the specific scenarios and sample numbers are shown in table 2.

2.3. Structure of the CNN

A CNN structure mainly includes: input layer, convolution layers, pooling layers, fully connected layer, output layer (softmax layer, classification layer and regression layer), and activation functions. In this study, Leaky ReLU [32] is used as the activation function, as shown in figure 8, where α is a very small value, usually 0.01. The optimizer, Adam [33], which combines the advantages of two optimization algorithms, AdaGrad [34] and RMSProp [35], is used. It has the advantages of simple implementation, efficient calculation, and lfewer memory requirements.

The ACC signals and the DIS signals are stored in a matrix of 400 × 7, the E signal is stored in a matrix of 400 × 60, and the fusion of the three signals is stored in a matrix of 400 × 74 (400, 7 + 7 + 60 = 74). Take the ACC signal as an example, since seven acquisition points of acceleration are set, the sampling time is 4 s, and the increment is 0.01 s, so each acquisition point will acquire 400 sampling points. In this study, the signals collected at each collection point are placed in columns to form a 400 × 7 matrix. The feature matrix of 397 × 6 is obtained through the first convolution layer (kernel number: 64, kernel size: 4 × 2), and then after maximum pooling layer (size 3 × 1, step size 1), the feature matrix of 395 × 6 is obtained. Then the second convolution (kernel number: 128, kernel size: 2 × 2) is carried out and the feature matrix of 394 × 5 is obtained. Finally, the feature matrix is mapped to the damage location of the structure through the softmax layer and the classification layer. The CNN structure and parameters are shown in figure 9 and table 3.

The output is the damage location. In this paper, for a single damage scenario, the label of the output damage location is set to 1, 2, …, 60, 61. If the output is 1, the prediction is an intact structure, and if the output is 2, damage to the No. 1 member is predicted, and so on. For double damage scenarios, the damage location is output in the form of a vector. For example, the vector ([0, 0.5, 0.5, 0, …, 0, 0, 0]) represents the damage of No. 2 and No. 3 members, and the damage degree is 50%, the vector ([0, 0, 0, 0.5, …, 0, 0, 0.5]) represents the damage of No. 4 and No. 60 members, and the damage degree is 50%, and so on.

The DLF is similar to the voting process, and the one with more votes wins. In this paper, the detection results are the ones in which more vibration signals vote. This method can effectively avoid the situation where the detection effect is not ideal when using one damage indicator. Four CNN models are trained by using four signals respectively, and the output results of the test samples from each network are fused at a decision level [36], which is implemented as follows:

$$F_i = [a_i, b_i, c_i, d_i] \tag{1}$$

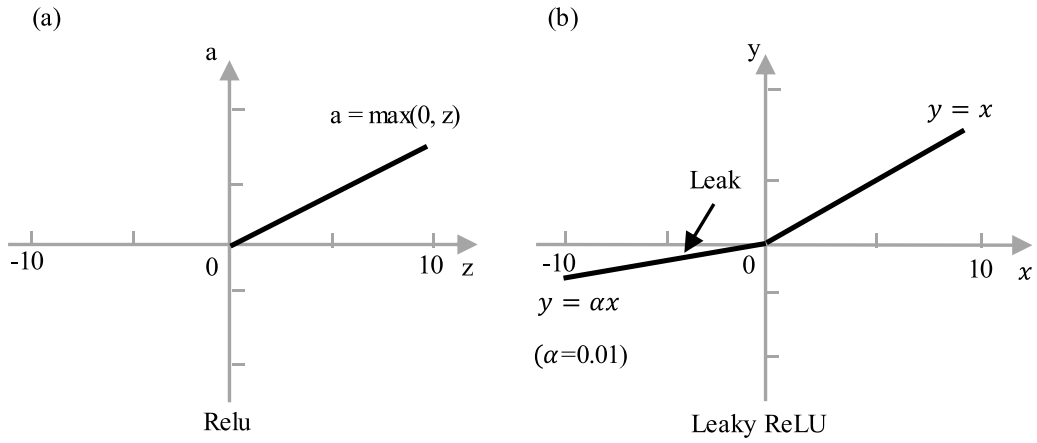

Figure 8. Function image: (a) ReLU, (b) Leaky ReLU.

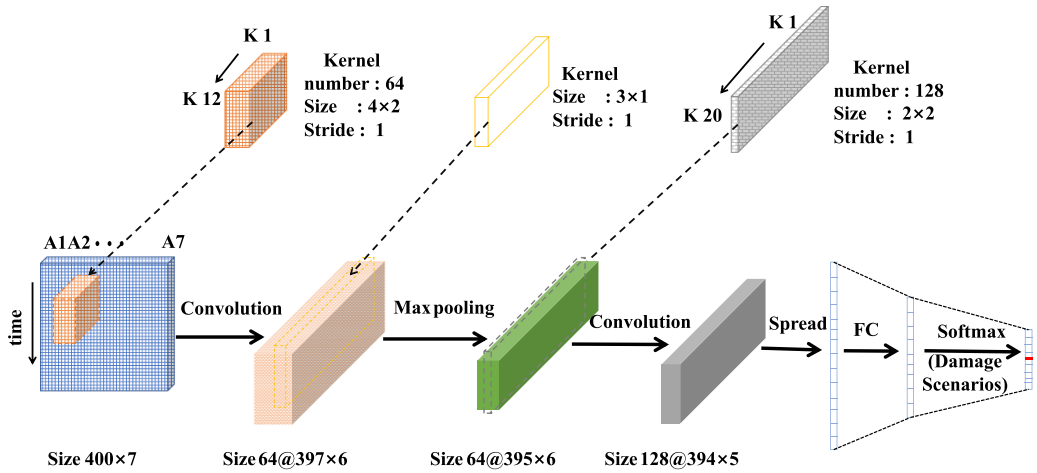

Figure 9. Structure of a CNN. FC: fully connected layer; #@$m \times n$: (#: kernel number; $m \times n$: size of the feature matrix).

Table 3. Parameters of a CNN.

Layer	Type	Kernels number	Kernels size	Step	Activation
1	Input	None	None	None	None
2	Convolution	64	4×2	[1, 1]	Leaky ReLu
3	Max pooling	None	3×1	[1, 1]	None
4	Convolution	128	2×2	[1, 1]	Leaky ReLu
5	FC	None	None	None	None
6	Softmax	None	None	None	None
7	Output	None	None	None	None

where $i = 1, 2, 3, 4$, and a_i, b_i, c_i, d_i are the detection results of the ith network in each type, the DLF is calculated according to the detection results of the four networks:

$$F_{\mathrm{D}} = \begin{bmatrix} F_1 \\ F_2 \\ F_3 \\ F_4 \end{bmatrix} = \begin{bmatrix} a_1 & b_1 & c_1 & d_1 \\ a_2 & b_2 & c_2 & d_2 \\ a_3 & b_3 & c_3 & d_3 \\ a_4 & b_4 & c_4 & d_4 \end{bmatrix} \tag{2}$$

$$\mathrm{DLF} = \mathrm{mode}(F_{\mathrm{D}}, 2) \tag{3}$$

where mode is a Matlab (MathWorks Inc., Providence, USA) function, which calculates the number with the highest frequency in each column, that is, the four networks vote on decisions, and the decision with the most votes is the final result. Figure 10 depicts an overview of the proposed DLF method.

3. Results and discussions

This section includes two parts: (a) based on the results of numerical simulations, the results of a single network are

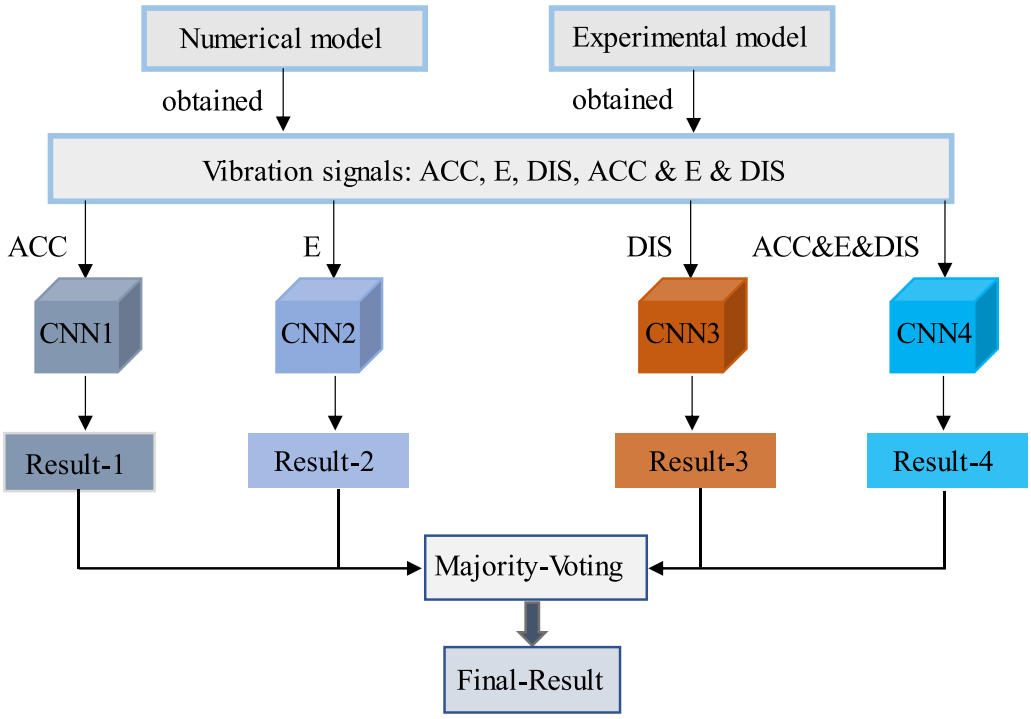

Figure 10. Overview of the methodology.

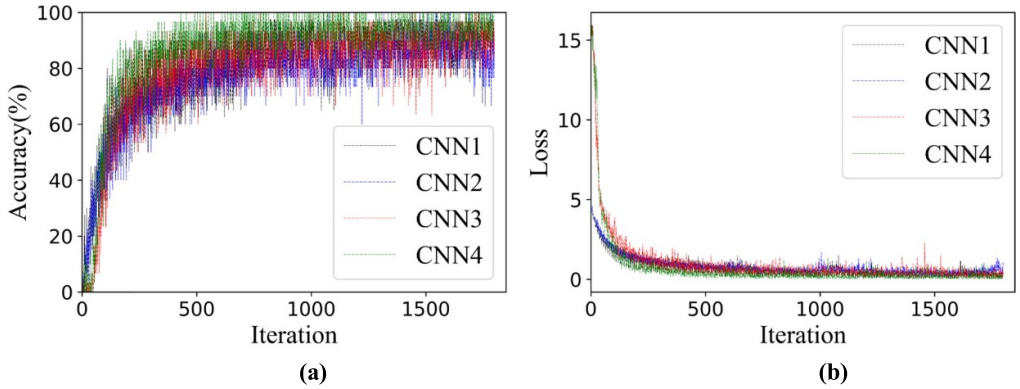

Figure 11. Training curves of CNNs: (a) accuracy curves; (b) loss curves.

compared with DLF; (b) based on the results of vibration experiments, it is validated that the result of DLF is better than that of a single network.

3.1. SDD results of numerical simulations

For the scenarios with a single damage, the training processes of these four networks (CNN1, CNN2, CNN3, and CNN4) are shown in figure 11. After 1800 iterations, the accuracy curves of the four networks reach convergence, and the loss values tend to be zero. Figure 12 shows the detection accuracy of these four CNNs. It can be seen that the CNN4 model has a higher prediction accuracy than the other three. Therefore, this paper divides the weights of the four CNN models according to their prediction performance, and the weights of CNN4, CNN3, CNN1, CNN2 are 0.4, 0.3, 0.2, 0.1 respectively. Table 4 lists the different detection results of the four CNNs for the same damage scenario.

According to the specific detection results listed in table 4, for S1 damage, the CNN1, CNN2, and CNN3 detect S39, while the CNN4 detects S1; for S7 damage, the detection result of the CNN1, CNN3 and CNN4 is S7, and the detection result of the CNN2 is S60; according to the aforementioned DLF strategy, the detection results of the four network models are fused. Therefore, for S1 damage and S7 damage, the final detection results are S1 and S7. A special scenario needs to be explained: for S47 damage, the CNN1 and CNN2 detect S39, while the CNN3 and CNN4 detect S47. When there are prediction results with the same number of votes, the CNN4 group is selected as the final decision result (according to the weights proposed above), that is, the final detection result is S47.

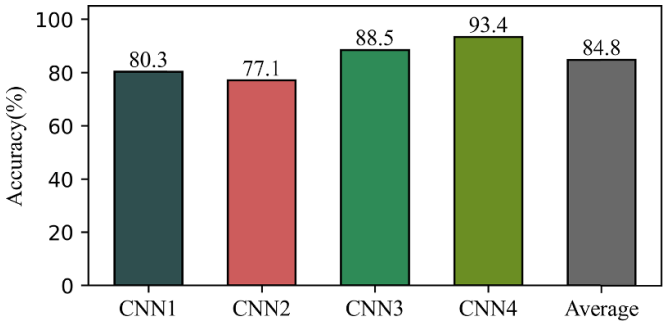

Figure 12. Detection accuracy of CNNs.

Table 4. Detection results of the four CNNs for the same damage scenario.

Actual damage (S)	Predicted damage (S)				Actual damage (S)	Predicted damage (S)			
	CNN1	CNN2	CNN3	CNN4		CNN1	CNN2	CNN3	CNN4
1	39	39	39	1	26	28	26	26	26
7	7	60	7	7	27	27	13	27	27
8	8	53	8	8	28	27	28	28	28
14	14	61	14	14	40	40	40	41	40
15	15	15	22	15	41	41	41	41	40
16	15	16	17	16	47	39	39	47	47
17	17	3	17	5	49	49	50	29	49
18	49	18	58	18	53	53	8	53	53
19	20	4	19	19	57	45	57	57	57
20	20	44	20	20	58	58	45	58	58
21	19	21	21	21	59	59	34	59	59
22	22	7	22	22	60	7	60	60	60
23	23	23	53	23	61	61	61	60	61
24	24	24	24	21	—	—	—	—	—

Table 5. Comparisons of detection accuracy before and after DLF for scenarios with a single damage.

CNN type	Accuracy	DLF	Improvement
CNN1	80.3%	98.4%	18.1%
CNN2	77.1%		21.3%
CNN3	88.5%		9.9%
CNN4	93.4%		5.0%
Average	84.8%	—	13.6%

The results show that the detection accuracy of the DLF strategy reaches 98.4%, which is an average improvement of 13.6% in accuracy compared with the single network before the fusion, where the specific details are shown in table 5.

In order to further validate the effectiveness of the DLF strategy, a double damage scenario is set up. In the double damage scenarios, CNN predicts the damage degree value of each member, and then takes the member with the largest damage degree as the corresponding damage location. Figure 13 shows the process of the prediction results of four CNNs under the E1. The damage locations predicted by CNN1 are No. 6 and No. 41 members. The other three CNN predictions are the No. 3 and No. 6 members, and so on. Table 6 shows the different detection results of the four networks for the same damage scenario with double damages.

For double-damage scenarios, according to the DLF strategy, the results show that the accuracy rate reaches 100% after the DLF. Compared with the detection accuracy of the four single networks, the accuracy rate is increased by 20.5% on average. The specific situation is shown in table 7. The results demonstrate that the scenarios with double damages further validate that the SDD accuracy rate is improved by the DLF strategy.

3.2. SDD results of vibration experiments

The following only describes the excitation point P_3 in detail, and the other four excitation points only give the corresponding results. The vibration signals under different scenarios are obtained through vibration experiments. Figures 14 and 15 are the acceleration time history curves of the seven points and the strain time history curves of 11 bars collected under the intact scenario. Figure 16 is the displacement time history curves of the seven points.

Four CNN models are trained by samples described in table 2 in section 2.2. Figure 17 shows the training processes of the four networks. As the number of iterations increases, the accuracy rate increases, and the loss value decreases. When the number of iterations reaches 3600, the training curves finally converge. Figure 18 shows the average detection accuracy

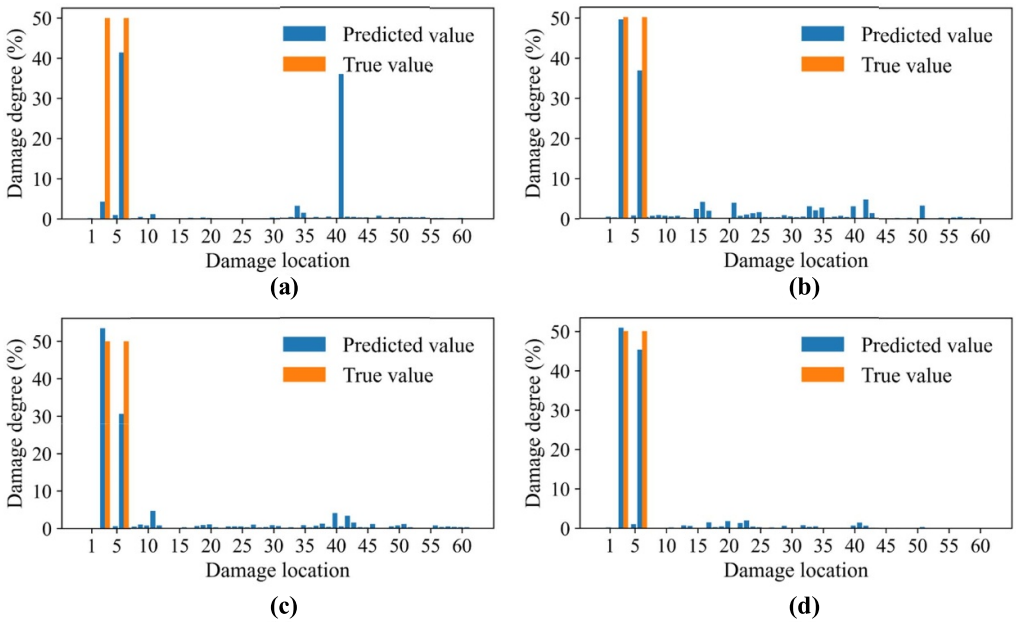

Figure 13. Process of prediction results of four CNNs under the E1: (a) CNN1, (b) CNN2, (c) CNN3, (d) CNN4.

Table 6. Damage detection of four types of CNNs.

Actual damage (S)	Predicted damage (S)				Actual damage (S)	Predicted damage (S)			
	CNN1	CNN2	CNN3	CNN4		CNN1	CNN2	CNN3	CNN4
E1	6,41	3,6	3,6	3,6	E7	18,35	18,19	18,20	18,19
E4	5,25	3,33	3,25	3,24	E8	35,55	35,40	35,40	35,40
E5	11,34	3,34	3,34	3,34	E11	40,43	41,43	41,43	41,43
E6	11,34	5,34	5,34	5,11	—	—	—	—	—

Table 7. Comparisons of detection accuracy for double damages before and after DLF.

CNN type	Accuracy	DLF	Improvement
CNN1	54.5%	100%	45.5%
CNN2	90.9%		9.1%
CNN3	81.8%		18.2%
CNN4	90.9%		9.1%
Average	79.5%		20.5%

rates of four CNNs in scenario 1 to scenario 6. Tables 8–11 show the specific detection results of the four CNNs in each scenario, respectively.

Due to the large number of samples (3612 samples), table 12 only presents the detection errors for some of the scenarios of CNN1, CNN2, CNN3 and CNN4.

According to the proposed DLF strategy, the predicted results of the four networks are fused. The results show that the average accuracy rate of scenario 1 to scenario 6 using the DLF strategy is 96.8%, and it is 5%–25.9% higher than that of a single network (table 13).

The prediction results for the excitation point P_3 are described in detail above. Table 14 lists the average prediction accuracy of five excitation points (P_1, P_2, P_4, P_3 and P_5) in six scenarios (SD1, SD2, SD3, SD4, SD5, SD6).

Table 14 demonstrates that damage detection is related to excitation points, and the influence of the excitation points on the prediction results of a single network is smaller than that on the DLF results. However, no matter which excitation point is considered, the prediction accuracy is improved with the DLF.

In summary, the result using DLF is better than the result of a single network. The scenarios with a single damage and double damages in numerical simulations and the various scenarios in the vibration experiments validate that the proposed method can effectively improve the accuracy of damage detection.

3.3. Discussions

In this paper, a supervised DL algorithm is used for SDD, and a DLF strategy is combined to improve the detection accuracy. Numerical simulations and vibration experiments are investigated to demonstrate the feasibility of the method. The limitations of this study are as follows.

Supervised learning algorithms need a large amount of labeled data, which is difficult or expensive to collect. In recent years, with the development of artificial intelligence, unsupervised learning [37, 38], semi-supervised learning [39], and active learning [40] have been widely applied in the field of SHM. On the other hand, since the damage to structures is complex, it is necessary to consider the influence of factors

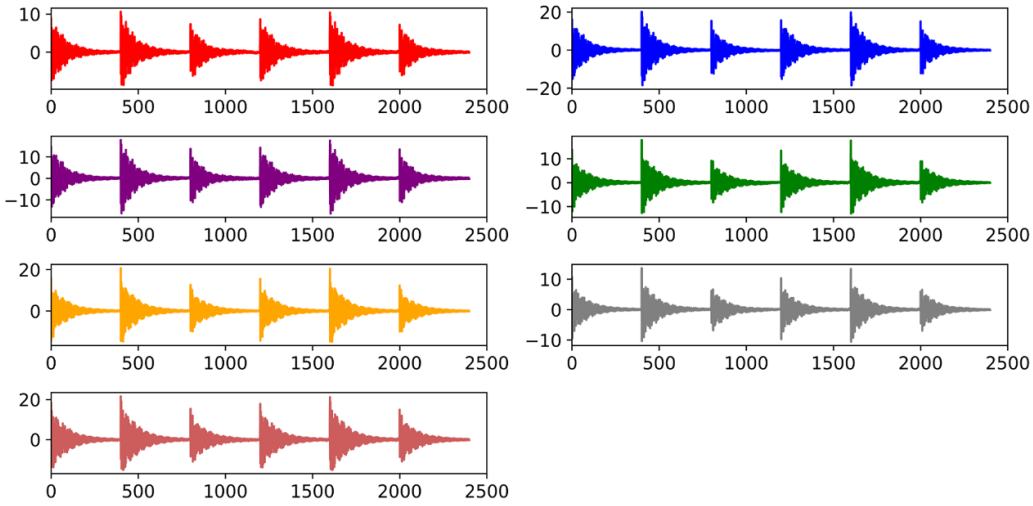

Figure 14. Acceleration time history curves of seven points.

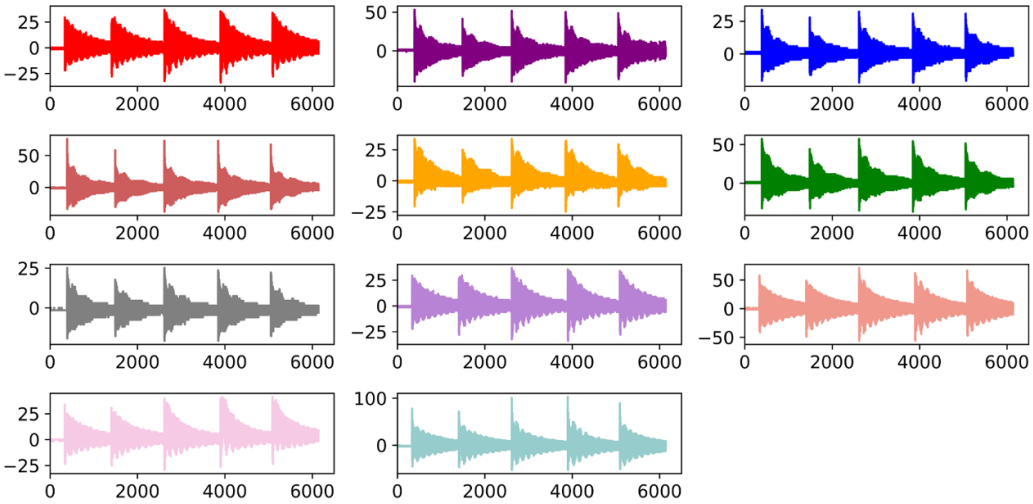

Figure 15. Strain time history curves of 11 bars.

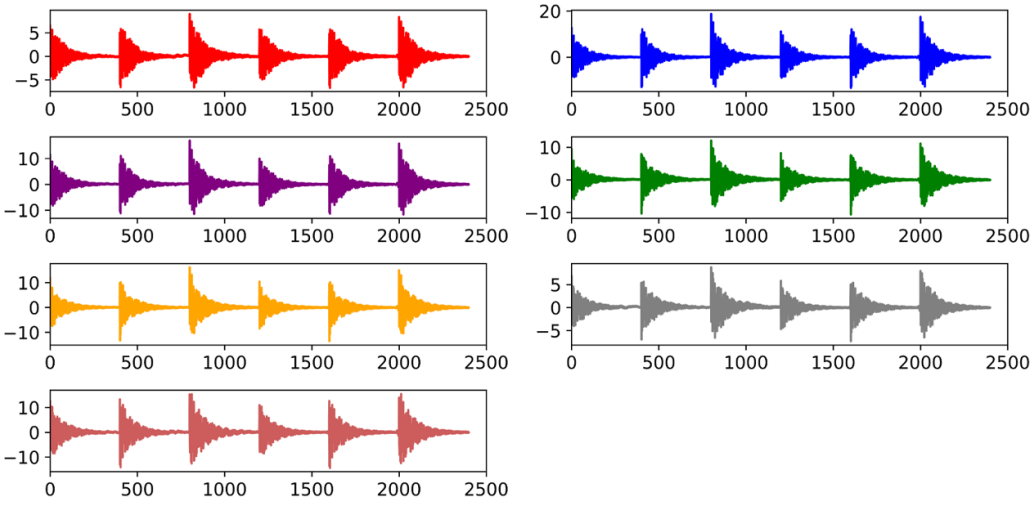

Figure 16. Displacement time history curves of seven points.

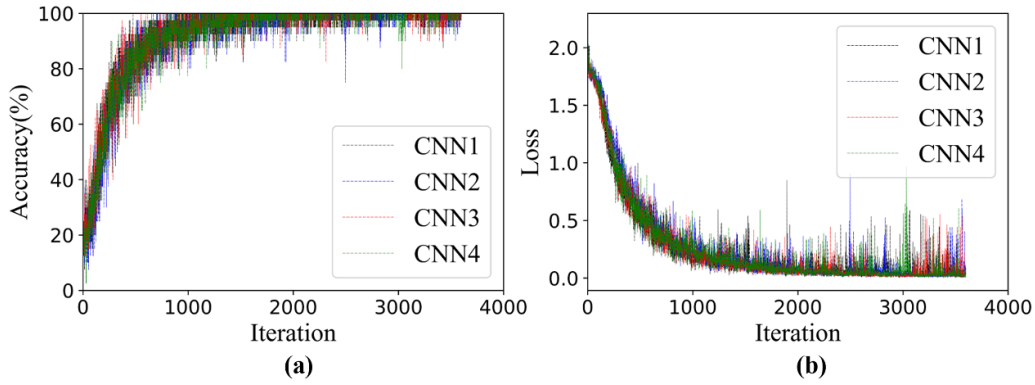

Figure 17. Training process of the four CNNs: (a) accuracy curves; (b) loss curves.

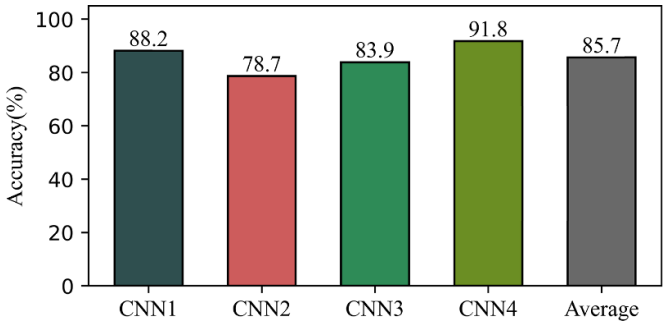

Figure 18. Average detection accuracy of CNNs in scenario 1 to scenario 6.

Table 8. Detection results of CNN1.

		Predicted damage scenario							
Damage scenario		1	2	3	4	5	6	Total	Accuracy
Damage scenario	1	507	95	0	0	0	0	602	84.2%
	2	23	567	0	2	6	4	602	94.2%
	3	1	82	503	13	3	0	602	83.6%
	4	0	0	0	600	2	0	602	99.7%
	5	0	0	0	0	602	0	602	100%
	6	0	3	0	177	16	406	602	67.4%
	Total	531	747	503	792	629	410	3612	88.2%

Table 9. Detection results of CNN2.

		Predicted damage scenario							
Damage scenario		1	2	3	4	5	6	Total	Accuracy
Damage scenario	1	124	478	0	0	0	0	602	20.6%
	2	124	478	0	0	0	0	602	79.4%
	3	0	80	462	55	5	0	602	76.7%
	4	2	41	0	509	50	0	602	84.6%
	5	0	33	17	20	511	21	602	84.9%
	6	0	24	0	1	100	477	602	79.2%
	Total	250	1134	479	585	666	498	3612	70.9%

such as load and environment, and so on. These challenges are indeed major ones facing SHM at present. The relevant scholars have proposed population-based methods (a large number of similar structures to analyze the common damage features of a population) and detect damages in similar structures.

In future work, the DLF method proposed in this paper will be combined with the population-based methods and other learning algorithms (unsupervised learning, semi-supervised learning, active learning) to improve its practicability.

Table 10. Detection results of CNN3.

Damage scenario		Predicted damage scenario						Total	Accuracy
		1	2	3	4	5	6		
Damage scenario	1	167	424	0	0	11	0	602	70.4%
	2	167	424	0	0	11	0	602	70.4%
	3	4	26	562	10	0	0	602	93.4%
	4	0	3	0	506	27	66	602	84.1%
	5	0	0	0	0	602	0	602	100%
	6	0	0	0	8	81	513	602	85.2%
	Total	338	877	562	524	732	579	3612	83.9%

Table 11. Detection results of CNN4.

Damage scenario		Predicted damage scenario						Total	Accuracy
		1	2	3	4	5	6		
Damage scenario	1	500	102	0	0	0	0	602	83.1%
	2	59	523	0	0	1	19	602	86.9%
	3	0	1	591	10	0	0	602	98.2%
	4	0	0	0	597	0	5	602	99.2%
	5	0	0	48	2	529	23	602	87.9%
	6	0	2	0	87	0	513	602	85.2%
	Total	559	628	639	696	530	560	3612	91.8%

Table 12. Some incorrect detections of the four networks.

Actual damage (scenario)	Predicted damage (scenario)				Actual damage (scenario)	Predicted damage (scenario)			
	CNN1	CNN2	CNN3	CNN4		CNN1	CNN2	CNN3	CNN4
1	1	2	2	1	3	2	3	1	3
1	1	1	2	1	3	2	3	1	4
1	1	2	1	1	3	4	3	3	3
1	2	1	1	1	4	4	4	4	6
1	2	2	2	1	4	4	4	6	4
1	1	2	5	1	4	4	4	6	6
1	2	2	5	2	4	3	4	2	4
1	2	2	2	2	4	4	2	4	4
1	2	1	1	2	4	4	2	2	4
2	1	2	2	1	4	4	1	2	4
2	1	2	1	1	4	4	2	5	4
2	1	2	1	2	5	5	5	5	6
2	1	2	2	1	5	5	5	5	4
2	2	1	2	1	5	5	5	5	3
2	2	2	2	1	6	5	5	5	5
2	2	1	1	2	6	4	6	6	6
2	1	2	1	6	6	4	5	6	6
2	1	1	2	5	6	6	5	6	6
2	2	2	1	6	6	4	5	6	4
2	1	2	2	6	6	4	5	5	6
2	5	2	1	6	6	6	5	5	6
3	3	3	3	6	6	2	5	5	2
3	2	3	3	3	6	2	5	5	6
3	5	3	3	3	6	6	6	4	6
3	2	3	3	3	6	4	6	4	6
3	2	3	2	3	6	4	2	6	4

Table 13. Comparison of accuracy rates before and after DLF.

Scenario	CNN1	CNN2	CNN3	CNN4	DLF	Improvement
SD1	84.2%	20.6%	70.4%	83.1%	91.4%	7.2%–70.8%
SD2	94.2%	79.4%	70.4%	86.9%	96.3%	2.1%–25.9%
SD3	83.6%	76.7%	93.4%	98.2%	100%	0.2%–23.3%
SD4	99.7%	84.6%	84.1%	99.2%	100%	0.3%–15.9%
SD5	100%	84.9%	100%	87.9%	100%	0%–15.1%
SD6	67.4%	79.2%	85.2%	85.2%	93.1%	7.9%–25.7%
Average	88.2%	70.9%	83.9%	91.8%	96.8%	5%–25.9%

Table 14. Average prediction accuracy after DLF in six scenarios.

Excitation point	CNN1	CNN2	CNN3	CNN4	DLF	Improvement
P_1	81.3%	68.9%	80.1%	86.5%	95.3%	8.8%–26.4%
P_2	86.5%	66.9%	77.1%	89.3%	95.6%	6.3%–28.7%
P_3	88.2%	70.9%	83.9%	91.8%	96.8%	5%–25.9%
P_4	85.3%	68.5%	81.6%	88.4%	96.4%	8%–27.9%
P_5	82.4%	69.3%	75.6%	92.2%	94.2%	2%–24.9%

4. Conclusions

Based on DLF strategy, the detection results of each CNN model are fused to obtain the final detection results.

From the above discussions, the following conclusions can be drawn:

(a) In the numerical simulations, the scenarios with a single damage and double damages are used to validate the proposed DLF strategy. Compared with the detection results of a single network, the accuracy rate based on DLF strategy increases by 5%–21.3%, i.e. an average increase of 13.6%; for scenarios with double damages, the detection accuracy increases by 9.1%–45.5%, i.e. an average increase of 20.5%.
(b) Six damage scenarios are set up in the vibration experiments. The average accuracy rate after DLF is as high as 96.8%, which is 5%–25.9% higher than the accuracy of a single network.
(c) The results of the proposed DLF strategy are better than that of any single network.
(d) Damage detection based on multiple signals can more comprehensively reflect the structural state and avoid the disadvantages of a single signal.

Data availability statement

The data that support the findings of this study are available upon reasonable request from the authors.

Acknowledgment

The support from the Program of Study Abroad for Young Scholars in Guangdong University of Technology (Grant No. 220410009) is acknowledged.

Conflict of interest

The authors declare no conflict of interest.

ORCID iD

Gongfa Chen https://orcid.org/0000-0002-9814-8147

References

[1] Torzoni M, Rosafalco L, Manzoni A, Mariani S and Corigliano A 2022 SHM under varying environmental conditions: an approach based on model order reduction and deep learning *Comput. Struct.* **266** 106790
[2] Khuc T *et al* 2020 A non-parametric method for identifying structural damage in bridges based on the best-fit auto-regressive models *Int. J. Struct. Stab. Dyn.* **20** 2042012
[3] Avci O *et al* 2018 Wireless and real-time structural damage detection: a novel decentralized method for wireless sensor networks *J. Sound Vib.* **424** 158–72
[4] Pandey A K, Biswas M and Samman M M 1991 Damage detection from changes in curvature mode shapes *J. Sound Vib.* **145** 321–32
[5] Cha Y J and Buyukozturk O 2015 Structural damage detection using modal strain energy and hybrid multiobjective optimization *Comput. Aided Civ. Infrastruct. Eng.* **30** 347–58
[6] Teng S *et al* 2020 Structural damage detection using convolutional neural networks combining strain energy and dynamic response *Meccanica* **55** 945–59
[7] Sung S H, Koo K Y and Jung H J 2014 Modal flexibility-based damage detection of cantilever beam-type structures using baseline modification *J. Sound Vib.* **333** 4123–38
[8] Lu Q, Ren G and Zhao Y 2002 Multiple damage location with flexibility curvature and relative frequency change for beam structure *J. Sound Vib.* **253** 1101–14
[9] Nifutao F, Zhangjian J and Noorimohammad N 2019 Deep learning for data anomaly detection and data compression of a long-span suspension bridge *Comput. Aided Civ. Infrastruct. Eng.* **35** 685–700

[10] Ml A *et al* 2022 Structural damage identification using strain mode differences by the iFEM based on the convolutional neural network (CNN) *Mech. Syst. Signal Process.* **165** 108289
[11] Sun H Y and Wen F 2014 Structural damage identification method based on displacement data *Appl. Mech. Mater.* **610** 241–5
[12] Ghiasi R, Torkzadeh P and Noori M 2016 A machine-learning approach for structural damage detection using least square support vector machine based on a new combinational kernel function *Struct. Health Monit.* **15** 302–16
[13] Yam L H, Yan Y J and Jiang J S 2003 Vibration-based damage detection for composite structures using wavelet transform and neural network identification *Compos. Struct.* **60** 403–12
[14] Mehrjoo M *et al* 2008 Damage detection of truss bridge joints using artificial neural networks *Expert Syst. Appl.* **35** 1122–31
[15] Gonzalez M P and Zapico J L 2008 Seismic damage identification in buildings using neural networks and modal data *Comput. Struct.* **86** 416–26
[16] Chun P J, Yamashita H and Furukawa S 2015 Bridge damage severity quantification using multipoint acceleration measurement and artificial neural networks *Shock Vib.* **2015** 789384
[17] Lautour O and Omenzetter P 2010 Damage classification and estimation in experimental structures using time series analysis and pattern recognition *Mech. Syst. Signal Process.* **24** 1556–69
[18] Peeters B *et al* 2004 The PolyMAX frequency-domain method: a new standard for modal parameter estimation? *Shock Vib.* **11** 523692
[19] Katunin A, Santos J and Lopes H 2021 Damage identification by wavelet analysis of modal rotation differences *Structures* **30** 1–10
[20] Dackermann U, Li J and Samali B 2009 Damage identification in timber bridges utilising the damage index method and neural network ensembles *Aust. J. Struct. Eng.* **9** 181–94
[21] Kiranyaz S *et al* 2018 Real-time fault detection and identification for MMC using 1D convolutional neural networks *IEEE Trans. Ind. Electron.* **66** 8760–71
[22] Ciresan D C *et al* 2010 Deep, big, simple neural nets for handwritten digit recognition *Neural Comput.* **22** 3207–20
[23] Zhong K *et al* 2020 Structural damage features extracted by convolutional neural networks from mode shapes *Appl. Sci.* **10** 4247
[24] Lin Y Z, Nie Z H and Ma H W 2017 Structural damage detection with automatic feature-extraction through deep learning *Comput. Aided Civ. Infrastruct. Eng.* **32** 1025–46
[25] Teng S *et al* 2021 Concrete crack detection based on well-known feature extractor model and the YOLO_v2 network *Appl. Sci.* **11** 813
[26] Chao Q *et al* 2022 Adaptive decision-level fusion strategy for the fault diagnosis of axial piston pumps using multiple channels of vibration signals *Sci. China Technol. Sci.* **65** 470–80
[27] Li S *et al* 2017 An ensemble deep convolutional neural network model with improved D-S evidence fusion for bearing fault diagnosis *Sensors* **17** 1729
[28] Tang Z *et al* 2019 Convolutional neural network-based data anomaly detection method using multiple information for structural health monitoring *Struct. Control Health Monit.* **26** e2296
[29] Ernesto G and Maura I 2014 A multi-stage data-fusion procedure for damage detection of linear systems based on modal strain energy *J. Civ. Struct. Health Monit.* **4** 107–18
[30] Huo Z *et al* 2020 Bearing fault diagnosis using multi-sensor fusion based on weighted D-S evidence theory vol 69 (*IEEE*) pp 2607–20
[31] Huo Z *et al* 2020 Entropy measures in machine fault diagnosis: insights and applications *IEEE Trans. Instrum. Meas.* **69** 2607–20
[32] Toth L S 2015 Phone recognition with hierarchical convolutional deep maxout networks *Eurasip J. Audio Speech Music Process.* **2015** 25
[33] Chandriah K K and Naraganahalli R V 2021 RNN/LSTM with modified Adam optimizer in deep learning approach for automobile spare parts demand forecasting *Multimed. Tools Appl.* **80** 26145–59
[34] Fan Z *et al* 2021 Detection and segmentation of underwater objects from forward-looking sonar based on a modified Mask RCNN *Signal Image Video Process.* **15** 1135–43
[35] Halgamuge M N, Daminda E and Nirmalathas A 2020 Best optimizer selection for predicting bushfire occurrences using deep learning *Nat. Hazards* **103** 845–60
[36] Zeng F *et al* 2019 Fault classification decision fusion system based on combination weights and an improved voting method *Processes* **7** 783
[37] Hassan Daneshvar M and Sarmadi H 2022 Unsupervised learning-based damage assessment of full-scale civil structures under long-term and short-term monitoring *Eng. Struct.* **256** 114059
[38] Sarmadi H and Yuen K-V 2022 Structural health monitoring by a novel probabilistic machine learning method based on extreme value theory and mixture quantile modeling *Mech. Syst. Signal Process.* **173** 109049
[39] Bull L A, Worden K and Dervilis N 2020 Towards semi-supervised and probabilistic classification in structural health monitoring *Mech. Syst. Signal Process.* **140** 106653
[40] Bull L A *et al* 2018 Active learning for semi-supervised structural health monitoring *J. Sound Vib.* **437** 373–88